Behavior of excess electrons in a one-dimensional classical bath: Equilibrium properties

Ashok Sethia and Yashwant Singh
Department of Physics, Banaras Hindu University, Varanasi 221 005, India
(Received 9 February 1990)

The behavior of an excess electron in a one-dimensional classical liquidlike bath is studied. A variety of equilibrium properties of the electron and the solvent are presented to characterize the structures of the different systems. For a repulsive potential between the electron and a fluid of hard rods, the electron becomes confined in a cavity. The localized electron exerts an "external field" on the solvent and creates ordered structures in it around the electron at high solvent densities. We find contrasting behavior for an electron rod potential in which a negative δ function is assumed to be situated at the center of each hard rod. For the force parameters taken in this calculation, the electron is found to exist in a "quasifree" state and forms a cluster of solvent particles around it. Ordered structure is found to develop in the cluster as the solvent density is increased.

I. INTRODUCTION

Excess electrons in deformable media exhibit a variety of phenomena.[1] In low-density gases, for example, the electron behaves almost like a free particle. As the gas density is increased, a variety of effects can substantially change the "bare" state of the electron. At liquid densities the electron may get trapped in a cavity or droplet of solvent particles created by its own field or remain "quasifree" depending upon the nature of the electron-solvent interactions. Observed properties such as the electron mobility[2] and absorption spectra[3] probe the nature of the electronic states in deformable materials and the phenomena of localization.[4]

When an electron is solvated in a polar liquid such as water or ammonia, the strong anisotropic electron-solvent interaction causes significant local modification of the equilibrium fluid structure.[5] The electron becomes localized in a small cavity because molecules in a solvation shell orient to create a potential minimum. Similar "bubblelike" structures are also found in liquid helium and neon.[6,7] The reason for this behavior is strong repulsion between electron and solvent, which results in the depletion of the solvent molecules from the region of the electron and forms a highly localized state of the electron. In both cases of localization, the electron adiabatically follows the slow changes in the deformation and therefore "feels" the instantaneous potential well, and maintains the stationary nature of the well and of the corresponding deformation of the medium with its field.

In many other nonpolar fluids[8-10] like Ar, CH_4, etc., the electron always remains in a state of high mobility (or quasifree). The electronic mobility of these fluids is comparable to those found in many semiconducting materials. An interesting density dependence of the mobility has, however, been observed in them. It shows a minimum near critical fluid density and a maximum at liquid density. All these features of a solvated electron can, in principle, be understood[11] on the basis of Chandler, Singh, and Richardson[12] theory.

The theory of Chandler, Singh, and Richardson[12] (CSR) is based upon the path-integral formulation of quantum theory which maps the behavior of the electron on to that of a classical isomorphic polymer.[13] The solvent-induced potential surface for the self-interaction of the isomorphic polymer is evaluated using an integral equation (e.g., reference interaction site model[12]) or density-functional approach.[14] With the known potential surfaces, the polymer statistics is solved using a variational principle that allows the determination of the electronic properties and the structure of the liquid near the electron. The theory has been found to be quantitatively accurate for the quasifree and trapped states, but less accurate in the region of transition from quasifree to localized states.[15,16] The width of the solvent density over which the transition takes place is found to be broader than those predicted by the computer simulations. All these calculations are in three-dimensional space. Electronic states in reduced dimensions are of considerable interest. For example, for a system of less than two spatial dimension, electrons are localized with an infinitesimal amount of disorder.[17]

The interest in problems of electron or phonon propagation in a one-dimensional (1D) random potential stems from the discovery and extensive experimental study of a certain class of organic or metallo-organic materials.[18] These materials exhibit strongly anisotropic, quasi-one-dimensional behavior attributed to the fact that they consist of long chains, weakly interacting with each other. In many of these, the presence of a random potential has been proposed in order to explain their behavior. In this paper we concentrate on the equilibrium behavior of an excess electron in a one-dimensional liquidlike bath. Time-dependent properties of this system will be reported in a future communication.

The paper is organized as follows: In Sec. II we briefly review the CSR theory in a form suitable for the one-dimensional system. The model systems considered here are described in Sec. III Results are presented and discussed in Sec. IV.

II. THEORY OF ELECTRON SOLVATION

Though the problem of excess electrons in liquids belongs to a general problem of electrons in disordered material, the liquid medium in many ways differs from that of solids. In liquids the constituent particles are not only free to relax but they can also diffuse and the local environment around the solute electron can be substantially different from that in a solid.

In CSR theory[12] the partition function Z for an electron in a bath of classical particles is written as the functional integral

$$Z=\iint Dx(t)\int\left[\prod_{j=1}^{N}dX_j\right]\exp(-\beta W[x(t),\{X_j\}])\ , \tag{1}$$

where, in the continuum limit,

$$W[x(t),\{X_j\}]=\frac{1}{\beta\hbar}\int_0^{\beta\hbar}dt[\tfrac{1}{2}m|\dot{x}(t)|^2+U_{es}(x(t),\{X_j\})]\ . \tag{2}$$

Here X_j denotes the position of jth solvent particle and N denotes their total number. The path for the electron $x(t)$, in an imaginary time interval $0\lesssim t\lesssim\beta\hbar$, is periodic, i.e., $x(0)=x(\beta\hbar)$, U_{es} is the total potential energy of electron with solvent. The partition function Z is isomorphic to that for a solvated classical Gaussian ring polymer with interaction sites connected by a nearest-neighbor harmonic potential with the force constant $P/\beta\lambda_e^2$. Here P is number of interaction sites on the polymer and $\lambda_e=(\beta\hbar^2/m)^{1/2}$ is the thermal wavelength of the electron, λ_e is one of the lengths which characterize the system. The other relevant lengths are the solvent atom diameter σ, a length d which characterizes the electron-atom interaction and ρ_S^{-1} (ρ_S being the mean number density of the solvent).

When integrations are performed over variables $\{X_j\}$ with isomorphic polymer coordinates held fixed, Eq. (1) reduces[12,14] to

$$Z=e^{-\beta\Delta\mu}=\iint Dx(t)s^{(0)}[x(t)]y[x(t)]\ , \tag{3}$$

where

$$s^{(0)}[x(t)]\propto\exp\left[-\frac{1}{\hbar}\int_0^{\beta\hbar}dt\tfrac{1}{2}m|\dot{x}(t)|^2\right] \tag{4}$$

and

$$y[x(t)]=\exp\{-\beta\Delta\mu[x(t)]\}\ . \tag{5}$$

In Eq. (3), $s^{(0)}[x(t)]$ contains the intrapolymer energetics and the weighting of a configuration is determined by $y[x(t)]$ which is a Boltzmann's factor for the solvent contribution to the potential of mean force for the interaction sites on the polymer. In the continuum limit,

$$-\beta\Delta\mu[x(t)]=\rho_s\int_0^1 d\lambda\hat{c}_{es}(0,\lambda\rho_S)-\tfrac{1}{2}(\beta\hbar)^{-2}\int_0^{\beta\hbar}dt\int_0^{\beta\hbar}dt'v(|x(t)-x(t')|), \tag{6}$$

where

$$v(|x(t)-x(t')|)=-\int dx'\int dx''c_{es}(x',t)\chi_{SS}(x',x'')c_{es}(x'',x,t) \tag{7}$$

and

$$\hat{c}_{es}(0,\lambda\rho_S)=\int dx\ c_{es}(x,\lambda\rho_S)\ .$$

Here x and t appear as independent coordinates, x is the distance between two sites and t measures the length along the contour of the polymer and

$$\chi_{SS}(x',x'')=\rho_S\delta(x'-x'')+\rho_S^2h_{SS}(x',x'')$$

is the density-density correlation function ("susceptibility") of the unperturbed bath. In Eq. (7) c_{es} is the electron-solvent direct pair-correlation function. Its value is determined from the equation

$$h_{es}(x)=\int dx'\int dx''\omega(|x-x'|)c_{es}(|x'-x''|)\chi_{SS}(x'')\ , \tag{8}$$

where

$$\omega(|x-x'|)=(\beta\hbar)^{-1}\int_0^{\beta}d(t-t')\omega(|x-x'|;t-t')\ . \tag{9}$$

Equation (8) is solved for c_{es} and h_{es} using suitable closure relation. The intrapolymer pair-correlation function appearing in Eq. (9) is defined as

$$\omega(x;t-t')=\langle\delta(|x(t)-x(t')|-x)\rangle\ . \tag{10}$$

This pair-correlation function describes the pair structure of the isomorphic classical polymer, and it is the equilibrium response function for the electron. Points on the isomorphic polymer do not, however, correspond to positions of the electron in real time. Once an analysis of $\omega(|x-x'|;t-t')$ is constructed, real-time correlation functions and the dynamic response function can be determined from an analytic continuation.[19]

Since all sites of a ring polymer on the average are equivalent, the site dependence disappears from Eq. (8) and only the zero-frequency component $\omega(x)$ of the equilibrium response function is required in Eq. (8). In the CSR theory, key role is played by the intrapolymer correlation function $\omega(x)$ and the electron to solvent pair-correlation function.

$$g_{es}(x)=1+h_{es}(x)=\rho_s^{-1}\left\langle\sum_j\delta(|X_j-x(t)|-x)\right\rangle\ . \tag{11}$$

Use has been made of Feynman's variational approach[20] to calculate $\omega(x,t-t')$ from the known potential surface $\Delta\mu[x(t)]$. An optimum harmonic reference functional is identified and the behavior of $\omega(x,t-t')$ is determined by that reference. The structure of the liquid near the isomorphic polymer is determined mostly by the average polymer correlation function $\omega(x)$. With this assumption and the known values of $\omega(x)$, the electron solvent correlation functions h_{es} and c_{es} are determined

from Eq. (8). In this respect the problem becomes isomorphic to that of determining at infinite dilution the structure of the solvent around a molecule whose internal structure is described by $\omega(|x-x'|)$.

As mentioned above, in Feynman's variational approach one seeks a quadratic functional that best approximates, the functional integral

$$Z=\iint Dx(t)\exp\{-\beta S[x(t)]\} , \tag{12}$$

where

$$\beta S[x(t)]=\frac{1}{\hbar}\int_0^{\beta\hbar} dt\{\tfrac{1}{2}m|\dot{x}(t)|^2+\beta\Delta\mu[x(t)]\} . \tag{13}$$

The most general form of a Gaussian functional is

$$Z_0=\iint Dx(t)\exp\{-\beta S_0[x(t)]\} , \tag{14}$$

where

$$S_0[x(t)]=\Gamma_0+\tfrac{1}{2}(\beta\hbar)^{-2}\int_0^{\beta\hbar}dt\int_0^{\beta\hbar}dt'\Gamma(t-t') \times|x(t)-x(t')|^2 . \tag{15}$$

Here $\Gamma(t-t')$ is a solvent-induced force constant between different sites on the electron polymer and Γ_0 merely determines the zero of the energy. The Bogoliubov inequality provides a bound for Z in terms of the average over the reference Gaussian weight

$$\ln Z\geq\ln Z_0-\beta\langle S-S_0\rangle . \tag{16}$$

The optimization leads to following equation for the correlation function for the intrapolymer correlation in k space:

$$\omega(k,\tau)=\exp[-\tfrac{1}{2}k^2R^2(\tau)] , \tag{17}$$

where $R^2(\tau)$ is the imaginary-time mean-square correlation function and is given by the following expression:

$$R^2(\tau)=\langle|x(t)-x(t')|^2\rangle =2\sum_n\frac{1}{\beta m\Omega_n^2+\gamma_n}[1-\cos(\Omega_n\tau)] . \tag{18}$$

Here $\tau=t-t'$, $\Omega_n=(2\pi n/\beta\hbar)$, and

$$\gamma_n=\frac{2}{\pi}\int_0^{\infty}dk\int_0^{\beta\hbar}d\tau(k)k^2[1-\cos(\Omega_n\tau)]\omega(k\tau) . \tag{19}$$

The mean-square displacement between particles half way around the polymer chain yields the correlation length

$$R=R(\tfrac{1}{2}\beta\hbar) . \tag{20}$$

When there is ground-state dominance, characteristic of compact state, the function $R^2(t-t')$ starts from zero at $t-t'=0$ and rapidly increases to its "saturation" value. The characteristic rise time τ of this initial (complex) time dependence is measure of the energy difference ΔE between the ground state and the first manifold of excited states

$$\Delta E\sim\hbar/\tau .$$

This, however, gives only a rough estimate of the excitation energy. For more accurate estimate, the real-time method is necessary.[21] In the CSR theory the average kinetic energy E_k of the electron is given by[22]

$$\langle E_k\rangle=\tfrac{1}{2}k_BT\left[1+\sum_{n\neq0}\frac{\gamma_n}{\beta m\Omega_n^2+\gamma_n}\right] . \tag{21}$$

The potential energy E_p is computed from the relation

$$\langle E_p\rangle=\rho_s\int_0^{\infty}u(x)g_{es}(x)dx , \tag{22}$$

where $u(x)$ is the attractive interaction between the electron and atom.

III. MODEL SYSTEMS

We consider a bath of hard rods of length σ distributed in one dimension. The pair interaction between rods is taken to be

$$U_{es}(X)=\infty \quad \text{for } X\leq\sigma \qquad =0 \quad \text{for } X>\sigma . \tag{23}$$

For this system the pair-distribution function is found exactly[23]

$$g(X^*)=\left[\frac{1}{\rho_S^*}\right]\sum_{S=1}\frac{\Theta(X^*-s)}{(1/\rho_S^*-1)(s-1)!} \times\left[\frac{X^*-s}{1/\rho_S^*-1}\right]^{s-1}\exp\left[-\frac{X^*-s}{1/\rho_S^*-1}\right] , \tag{24}$$

where Θ is a unit step function, $X^*=X/\sigma$ and $\rho_S^*=\rho_S\sigma$. The structure factor $S(k)=1+\rho_S h(k)$ is found to be

$$S(k\sigma)=1+\frac{\cos(k\sigma)-1-k\sigma(1/\rho_S^*-1)\sin(k\sigma)}{1-\cos(k\sigma)+\frac{1}{2}(k\sigma)^2(1/\rho_S^*-1)^2+(k\sigma)(1/\rho_S^*-1)\sin(k\sigma)} . \tag{25}$$

In Fig. 1, we plot the structure factor of the liquid for $\rho_S^*=0.5$, 0.7, and 0.9. The close-packed density for this system is 1. At $\rho_S^*=0.9$ the peaks are sharp and are separated by values of $k\sigma$ close to 2π.

The electron-atom interaction in real system has a strong repulsion at short distances due to orthogonality requirements between the wave functions of the core electrons in the solvent particle and that of the excess electron and an attraction at large distances. The latter contribution is due to polarization of electron cloud in an atom. The medium polarization may give rise to the many-body effect. However, in system of neutral atoms

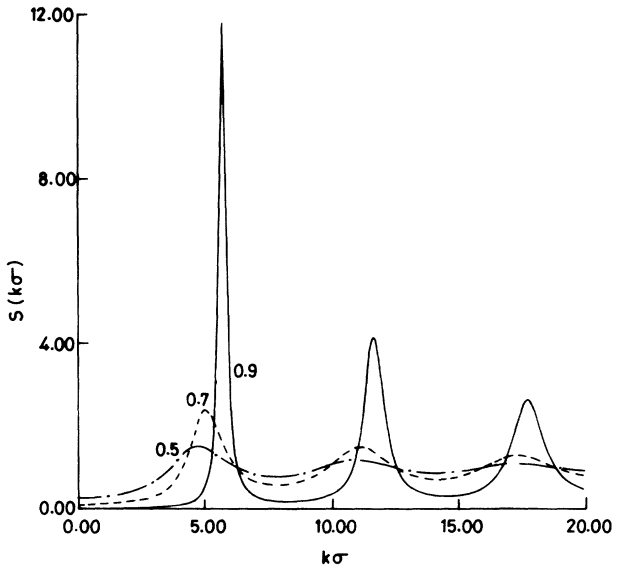

FIG. 1. Structure factor for the one-dimensional fluid of hard rods at $\rho_S^*=0.5$, 0.7, and 0.9.

the electronic states are determined primarily by the short-range repulsive interaction or excluded-volume effect. The attractive interactions become important only at low densities where the excess electron may induce cluster formation or affects the scattering cross sections.

In this article we present numerical results for two model potentials. In the first model we concentrate on the excluded volume effect on the electronic states, a model suitable for the study of excess electron in insulating media. The electron-atom interaction is taken to be hard rods with characteristic length d defined as

$$u_{es}(x)=\infty, \quad x\le d \ ,$$
$$=0, \quad x>d \ . \tag{26}$$

We take $d=\frac{1}{2}\sigma$.

In the second model, a negative δ-function potential is situated at the center of each hard rod

$$u_{es}(x)=-V_0\delta(x-X_n) \ , \tag{27}$$

where $V_0>0$ and X_n is the position of the nth ion. An isolated potential of this form leads to a bound state at the energy $E_0=-\frac{1}{4}V_0^2$. This represents a primitive model for the one-dimensional liquid metal. The hard rod prevents the overlapping of scatterers and implies short-range order as described by $g(X)$. Complete randomness is implied by $\rho_S^*\to 0$, a case which Klauder[24] treated in great detail and for which Frisch and Lloyd[25] obtained an exact solution. Strong correlation is implied by $\rho_S^*\sim 1$, and $\rho_S^*=1$ reduces the system to the familiar Kronig-Penney model. Results are given in terms of a dimensionless parameter

$$\epsilon=\frac{\rho_S\hbar^2}{mV_0}=\frac{\rho_S^*(\lambda_e/\sigma)^2}{\beta(V_0/\sigma)} \tag{28}$$

which measures the density relative to the potential strength. Our motivation for examining this model stems from the fact that an "exact" Monte Carlo calculation for the electronic density of states has been made by Peterson, Schwartz, and Butler.[26] Many approximate calculations have also been reported in the literature.[26,27]

We solve Eq. (8) for h_{es} and c_{es} for the first model using

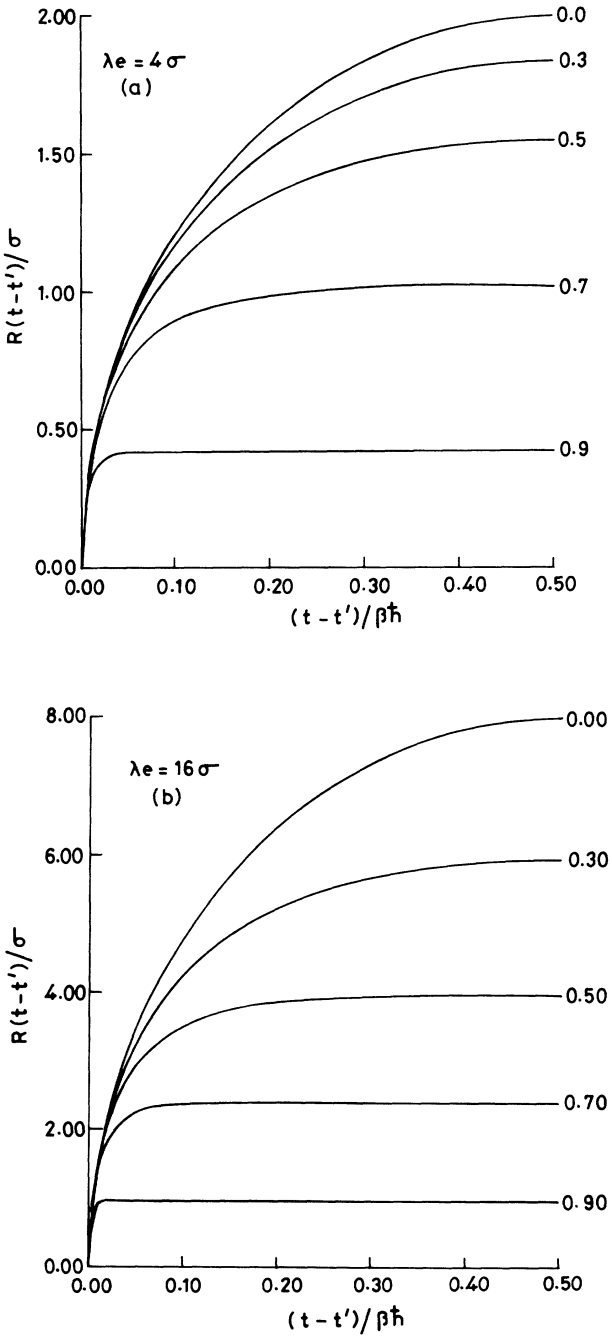

FIG. 2. Root-mean-square displacement as a function of Euclidean time for an excess electron in a fluid of hard rods interacting with fluid particles via a hard-rod potential (primitive model). The results are given for $d=\frac{1}{2}\sigma$ at (a) $\lambda_e=4\sigma$ and (b) $\lambda_e=16\sigma$ and several values of ρ_S^*. If $\sigma=5$ Å, the (a) and (b) curves would correspond to $T=221.2$ and 13.8 K, respectively.

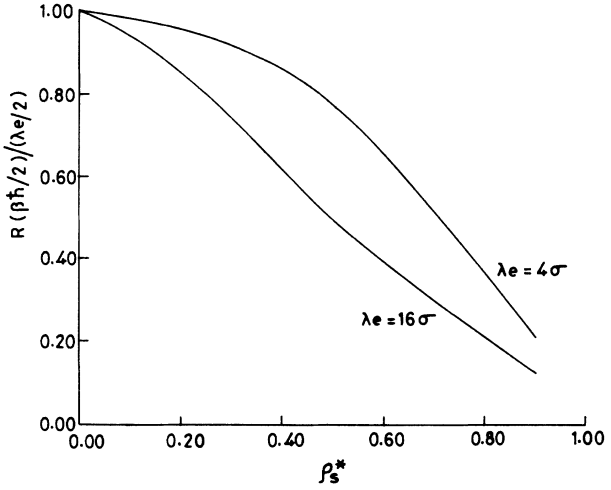

FIG. 3. Reduced correlation length of an electron in the one-dimensional fluid of hard rods for the primitive model as a function of solvent density at $\lambda_e=4\sigma$ and 16σ.

the closure relation

$$c_{es}(x)=0, \quad x>d \ ,$$

$$h_{es}(x)=-1, \quad x\lesssim d \ .$$

We can express Eq. (8) and the above closure relation in variational form as

$$0=\frac{\delta I_{\mathrm{RISM}}}{\delta c_{es}(x)}, \quad x\lesssim d \ ,$$

$$c_{es}(x)=0, \quad x>d \ , \tag{29}$$

where

$$I_{\mathrm{RISM}}=\rho_S\hat{c}_{es}(0)+\frac{1}{4\pi}\int_{-\infty}^{\infty} dk\,\hat{c}^{\,2}(k)\hat{\omega}(k)\hat{\chi}_{ss}(k) \ . \tag{30}$$

Equation (29) is solved numerically by expanding $c_{es}(x)$ for $x\leq d$ in a series of basis functions and then varying the coefficients of the basis functions. The details of the method are given elsewhere.[28]

For the second model we use the HNC closure relation

$$c_{es}(x)=h_{es}(x)-\ln[1+h_{es}(x)]-\beta u(x)$$

to solve Eq. (8). The self-consistency is achieved via a method described in Ref. 28.

IV. RESULTS AND DISCUSSIONS

The primary physical phenomenon we are looking for is the process of self-trapping of the electron. At low densities of the solvent, the electron polymer is fairly extended, fluctuating with nearly the free-particle Gaussian statistics where the second moment is given by

$$R^2_{\mathrm{free}}(t-t')=\lambda_e^2(t-t')(\beta\hbar-t+t')/(\beta\hbar)^2 \ .$$

The overall size of the isomorphic polymer is therefore

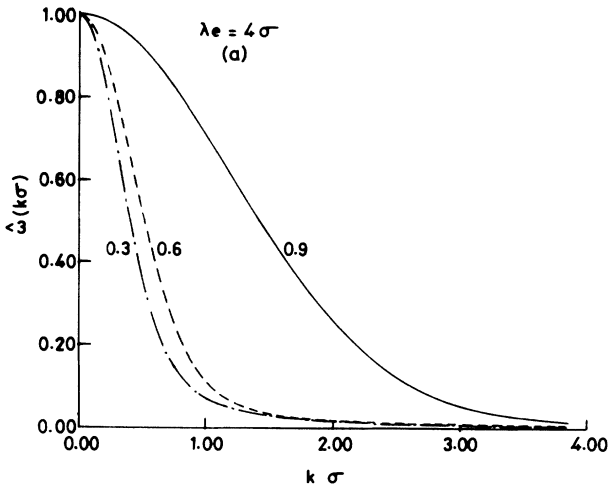

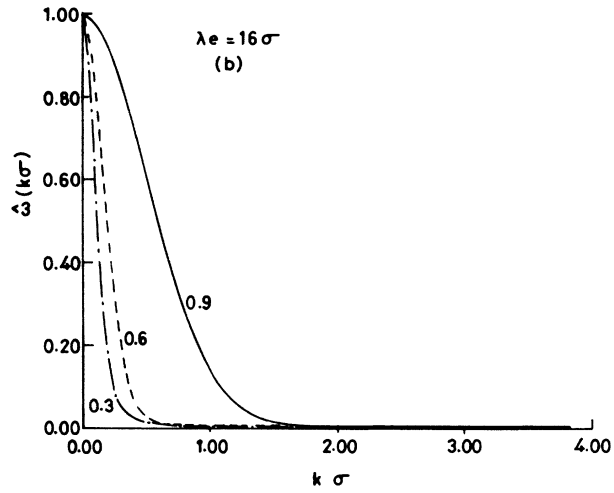

FIG. 4. The zero-frequency response function $\hat{\omega}(k\sigma)$ of an electron in the fluid of hard rods at three solvent densities $\rho_S^*=0.3$, 0.6, and 0.9 and (a) $\lambda_e=4\sigma$ and (b) $\lambda_e=16\sigma$.

roughly $\frac{1}{2}\lambda_e$. At high solvent densities, however, the packing of the fluid environments prohibits extended fluctuations, and the electron gets trapped occupying a region characterized by the length σ.

Since the interaction sites in the first model are excluded from penetrating spheres of radius d surrounding each particle, an electron is always localized between two adjacent scatterers. The localization length is function of the density of the solvent and the temperature. In the present model the temperature enters through λ_e which depends on β.

Our computed $R(t-t')$ correlation functions are illustrated in Figs. 2(a) and 2(b) for $\lambda_e/\sigma=4$ and 16, respectively, and at several solvent densities. At higher densities we find the characteristic *ground-state* dominance while, at lower densities, $R(t-t')$ is time dependent throughout the $0\leq t-t'\leq\beta\hbar$ interval. The temperature-dependent density which separates the two

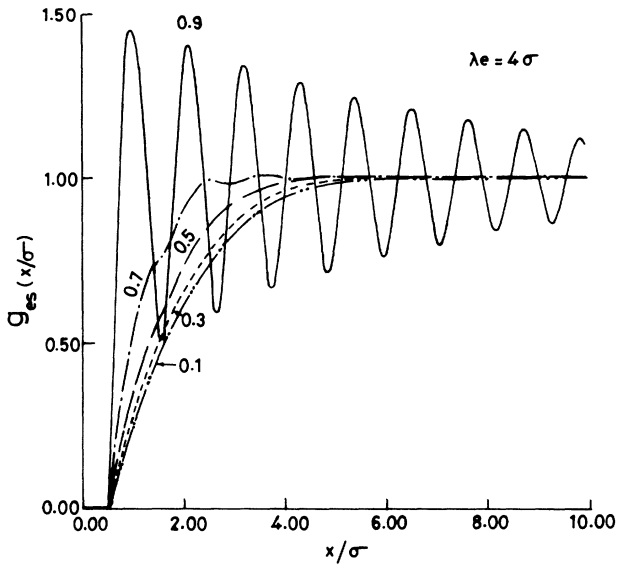

FIG. 5. The electron-solvent radial distribution function at $\lambda_e = 4\sigma$ and several solvent densities for the primitive model of an electron in a fluid of hard rods.

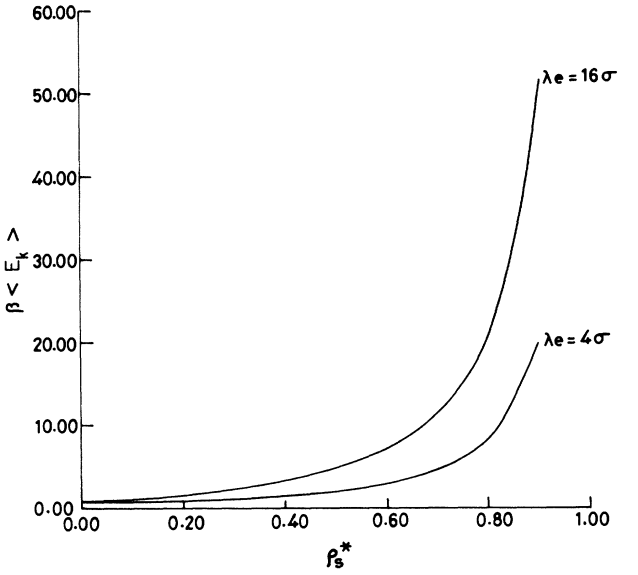

FIG. 7. Average kinetic energy of an excess electron in a fluid of hard rods interacting with fluid particles via the hard-rod potential as a function of solvent density. The result is given at $\lambda_e = 4\sigma$ and 16σ.

regimes can be found from this figure. The appearance of ground state is due to creation of trapped state by formation of a cavity for the electron.

The correlation length $R(\frac{1}{2}\beta\hbar)$ as a function of the solvent density for two temperatures is illustrated in Fig. 3. This length is related to the localization length. While for $\lambda_e \gg \sigma$, we find that $R(\frac{1}{2}\beta\hbar)$ varies almost linearly with ρ_S^{*-1}, for $\lambda_e \geq \sigma$ it remains almost constant at low densities and then varies almost linearly with ρ_S^{*-1}. This is in accordance with the picture of localization discussed above and differs qualitatively from that of the three-dimensional case.

Another quantity which sheds light on the behavior of the electron in the bath is the variation with the density of the response function $\hat{\omega}(k\sigma)$. We plot $\hat{\omega}(k\sigma)$ as a function of wave vector $k\sigma$ at several densities in Figs. 4(a) and 4(b). Because of the particle conservation,

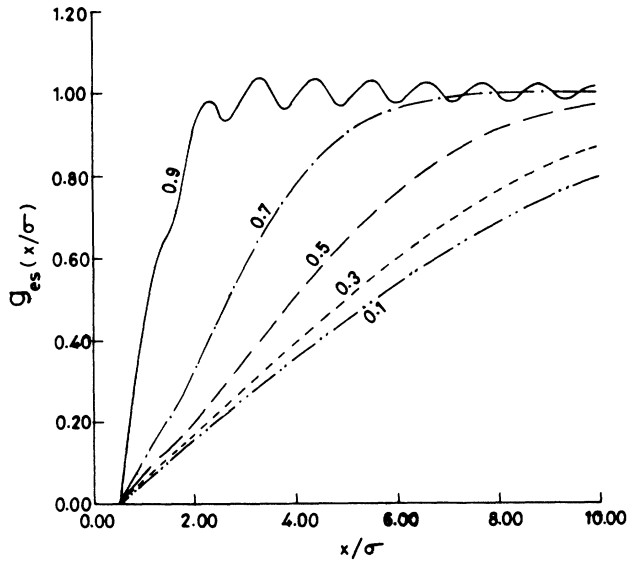

FIG. 6. Same as in Fig. 5 but for $\lambda_e = 16\sigma$.

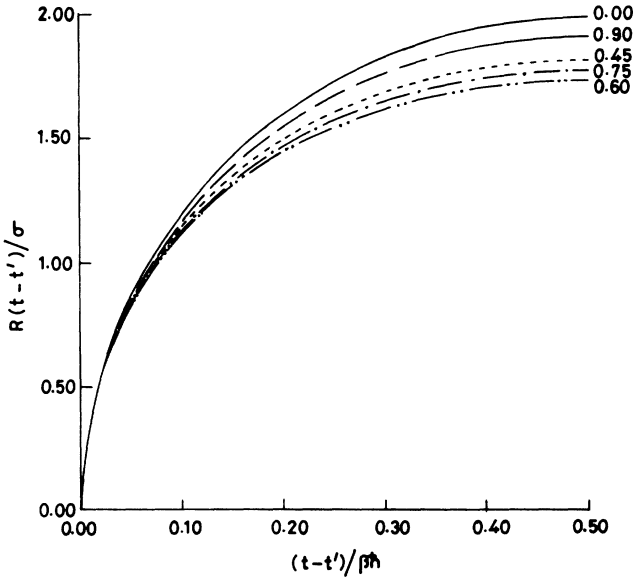

FIG. 8. Root-mean-square distance as a function of Euclidean time for the electron-atom potential model which has a negative δ function at the center of each rod (δ-potential model) at several values of ρ_S^* and $\epsilon = 1$ (see text for the definition of ϵ).

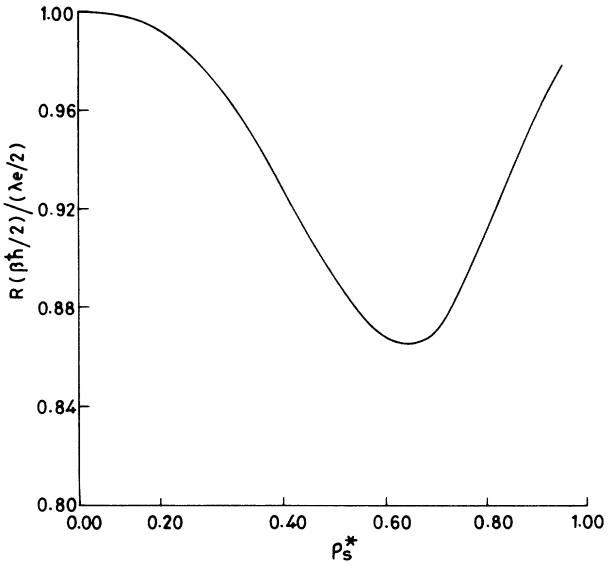

FIG. 9. Reduced correlation length of an electron in one-dimensional fluid of hard rods as a function of solvent density at $\epsilon=1$ for the δ-potential model.

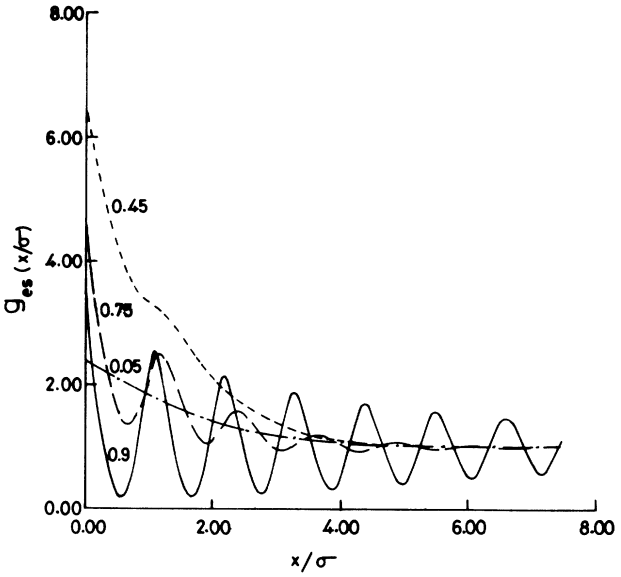

FIG. 11. The electron-solvent radial distribution function at several solvent densities for the δ-potential model at $\epsilon=1$.

$\hat{\omega}(0)=1$. At higher densities, as the ground-state dominance appears, $\hat{\omega}(k\sigma)$ becomes more broad indicating a more localized wave packet associated with the electron in real space.

Let us now consider the nature of the electron-solvent pair structure shown in Figs. 5 and 6. The behavior illustrates that the electron paths tend to expel solvent particles from the vicinity of the electron and forms the cavity in which it gets trapped. The size of the cavity can be estimated from these figures. It can also be inferred from these figures that the localized electron behaves like a soft sphere at low solvent density but becomes sufficiently hard to create local freezing at higher solvent densities. This freezing becomes more clear at higher temperatures, i.e., at $\lambda_e=4\sigma$ than $\lambda_e=16\sigma$. The external field needed to create such a density profile of the solvent is exerted by the trapped electron. In Fig. 7, we plot the kinetic energy of the electron as a function of densities at these two

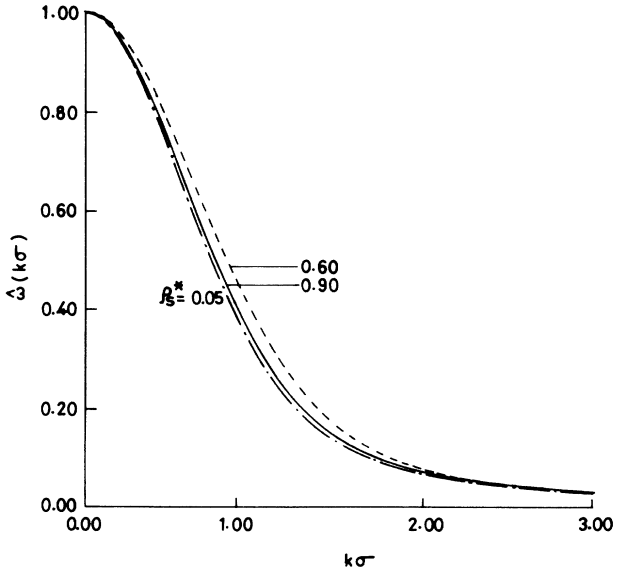

FIG. 10. The zero-frequency response function $\hat{\omega}(k\sigma)$ for the δ-potential model of three solvent densities mentioned in this figure and $\epsilon=1$.

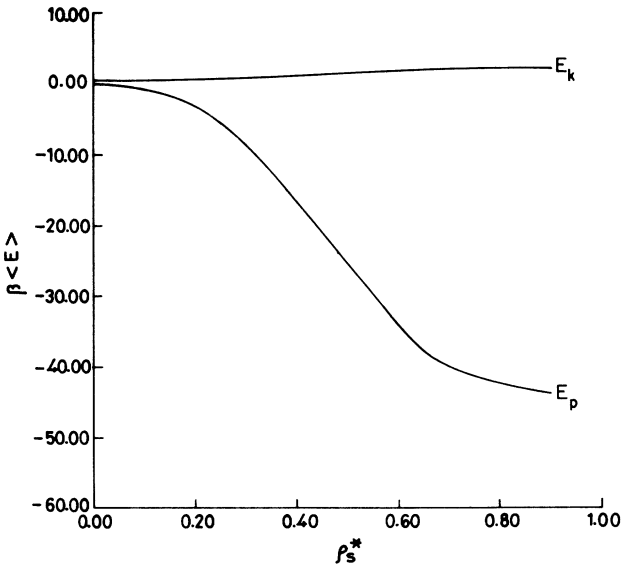

FIG. 12. Average kinetic and potential energies of the excess electron as a function of the solvent density for the δ-potential model and $\epsilon=1$.

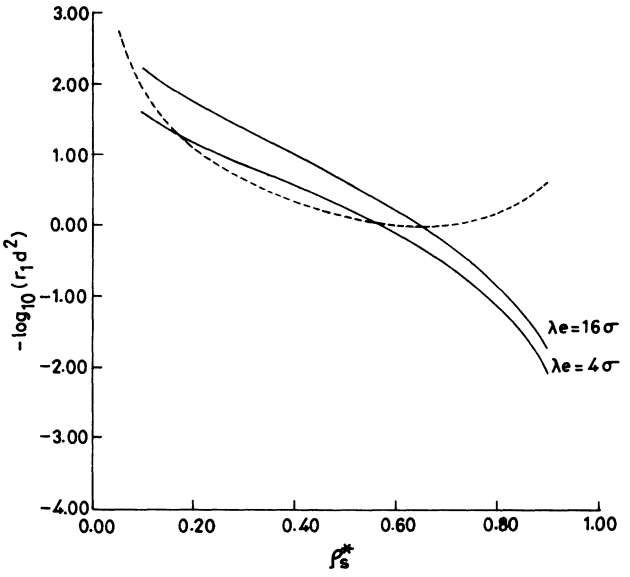

FIG. 13. Logarithm of the friction constant as a function of the solvent density for the primitive model (at two temperatures indicated by the solid lines) and the δ-potential model (the dotted line).

temperatures.

A different scenario is found in the case of the second model. The computed $R(t-t')$ correlation functions illustrated in Fig. 8 for $\epsilon=1$, $\lambda_e/\sigma=4$, and several solvent densities show that the electron polymer is always fairly extended, fluctuating with nearly the free-particle Gaussian statistics. The overall size of the isomorphic polymer is roughly $\frac{1}{2}\lambda_e$. This feature is more clear in Fig. 9 in which we plot the correlation length $R(\frac{1}{2}\beta\hbar)$ as a function of solvent density. We find that this length initially decreases as the solvent density is increased, has a minimum at about $\rho_S^*\sim 0.6$, and then increases. This minimum is, however, weak and does not change, in any significant way, the basic features of the isomorphic polymer. For small values of ϵ the minimum may be strong, greatly affecting the behavior of the electron.

In Fig. 10 we plot $\hat{\omega}(k\sigma)$ as a function of the wave vector $k\sigma$ at several densities. As expected, this function remains almost unaffected by the solvent density. Interesting structures can, however, be seen in the electron-solvent pair-correlation function $g_{es}(x)$ plotted in Fig. 11 for several solvent densities. We find that the electron due to attractive electron-atom interaction forms a cluster of solvent particles, with density distribution $\rho_c^*(x)=\rho_s^* g_{es}(x^*)$. The cluster initially becomes compact as the solvent density is increased. But, at about $\rho_S^*\sim 0.6$, the cluster expands and develops local structure. The structure in the cluster becomes very apparent at $\rho_S^*=0.9$.

In Fig. 12 we plot the average kinetic and potential energy of the solvated electron as a function of the liquid density. We see that while the kinetic energy remains almost constant at all densities, the potential energy decreases with density reaching to a saturation value. As has been emphasized before,[28] γ_1 is related to inverse mobility for the electron. A graph of $\log_{10}(1/\gamma_1)$ is given in Fig. 13 for both models. It indicates that, for the model of hard rods for the electron-atom interaction, the theory predicts a large variation of mobility as a function of density with almost linear behavior. But for the model in which electron-atom interaction is represented by an attractive δ peak, the mobility decreases initially reaching a minimum and then has the tendency of increasing with density. The real-time behaviors of these models are being investigated and will be reported soon.

ACKNOWLEDGMENTS

One of us (Y.S.) thanks David Chandler and T. V. Ramakrishnan for many stimulating discussions on this subject. The research was supported by Department of Science and Technology (New Delhi).

[1]See, for example, H. T. Davis and R. Brown, Adv. Chem. Phys. **31**, 329 (1975); D. Emin, Phys. Today **35**, 34 (1982).

[2]See, for example, N. E. Cipollini and A. O. Allen, J. Chem. Phys. **67**, 131 (1977); S. S. S. Huang and G. R. Freeman, *ibid.* **68**, 1355 (1978); Phys. Rev. A **24**, 714 (1984); F. M. Jacobsen, N. Gee, and G. R. Freeman, *ibid.* **34**, 2329 (1986).

[3]See, for example, B. Baron, P. Delahay, and P. Lugo, J. Chem. Phys. **57**, 2122 (1972); L. Kevan, *ibid.* **56**, 838 (1972); D. C. Walker, Can. J. Chem. **55**, 1987 (1977).

[4]N. F. Mott and E. A. Davis, *Electronic Processes in Noncrystalline Materials* (Clarendon, Oxford, 1971); D. J. Thouless, Phys. Rep. **13**, 91 (1974).

[5]J. Jortner and A. Gaathan, Can. J. Chem. **55**, 1801 (1977); P. Krebes, J. Phys. Chem. **88**, 3702 (1984); F.-Y. Jou and G. R. Freeman, *ibid.* **85**, 629 (1981).

[6]K. W. Schwartz, Phys. Rev. Lett. **41**, 239 (1978).

[7]J. L. Levine and T. M. Sanders, Phys. Rev. **154**, 138 (1967); A. J. Bartels, Appl. Phys. **8**, 59 (1975).

[8]J. A. Jahnke, L. Meyer, and S. A. Rice, Phys. Rev. A **3**, 734 (1971).

[9]S. S. S. Huang and G. R. Freeman, J. Chem. Phys. **68**, 1355 (1978).

[10]M. A. Floriano and G. R. Freeman, J. Chem. Phys. **85**, 1603 (1986).

[11]D. Laria and D. Chandler, J. Chem. Phys. **87**, 4088 (1987).

[12]D. Chandler, Y. Singh, and D. M. Richardson, J. Chem. Phys. **81**, 1975 (1984).

[13]D. Chandler and P. G. Wolynes, J. Chem. Phys. **74**, 4078 (1981).

[14]Y. Singh, J. Phys. A **20**, 3949 (1987).

[15]M. Sprik, M. L. Klein, and D. Chandler, J. Chem. Phys. **83**, 3042 (1985).

[16]D. F. Coker, B. J. Berne, and D. Thirumalai, J. Chem. Phys. **86**, 5689 (1987).

[17]E. Abrahams, P. W. Anderson, D. C. Licciardello, and T. V. Ramakrishnan, Phys. Rev. Lett. **42**, 673 (1979); S. John, H. Sompolinsky, and M.J. Stephen, Phys. Rev. B **27**, 5592 (1983).
[18]A. N. Bloch, R. B. Weisman, and C. M. Varma, Phys. Rev. Lett. **28**, 753 (1972); P. F. Williams and A. N. Bloch, Phys. Rev. B **10**, 1097 (1974); C. Papatriantafillou, E. N. Economou, and T. P. Eggarter, *ibid.* **13**, 910 (1976); R. Johnston and B. Kramer, Z. Phys. B **63**, 273 (1986).
[19]A. L. Nichols III and D. Chandler, J. Chem. Phys. **87**, 6671 (1987).
[20]R. P. Feynman, Phys. Rev. **97**, 660 (1957); *Statistical Mechanics* (Benjamin, New York, 1982).
[21]Y. Singh, S. Sanyal, and A. Sethia (unpublished); A. Sethia, S. Sanyal, and Y. Singh, J. Chem. Phys. (to be published).
[22]G. Malescio and M. Parrinello, Phys. Rev. A **35**, 897 (1987).
[23]Z. W. Salsburg, R. W. Zwanzig, and J. C. Kirkwood, J. Chem. Phys. **21**, 1098 (1953).
[24]J. R. Klauder, Ann. Phys. (N.Y.) **14**, 43 (1981).
[25]H. Frisch and S. Lloyd, Phys. Rev. **120**, 1175 (1960).
[26]H. K. Peterson, L. Schwartz, and W. H. Butler, Phys. Rev. B **11**, 3678 (1975).
[27]V. A. Singh and L. M. Roth, Phys. Rev. B **15**, 3694 (1977).
[28]A. L. Nichols III, D. Chandler, Y. Singh, and D. M. Richardson, J. Chem. Phys. **81**, 5109 (1984).